Nonideal Effects of Reconstruction Filter and I/Q Imbalance in Digital Predistortion

M. Y. Li, J. X. Deng, L. E. Larson and P. M. Asbeck

University of California, San Diego, La Jolla, CA 92093-0409

mili@ucsd.edu

Abstract — **Digital predistortion linearization results are often degraded by nonideal factors in the transmitter chain. Among them, the gain ripple and phase delay of the analog reconstruction filter and the gain and phase imbalance of quadrature modulator are the major sources of linearizer performance degradation. The paper studies these effects and presents general guidelines for filter selection and imbalance compensation to maximize the predistortion performance.**

Index Terms — **Nonlinear distortion, filters, transmitters, power amplifiers.**

I. Introduction

Digital predistortion techniques [1] for linearity improvement of transmitters have been extensively investigated in wireless communication systems, such as WCDMA, CDMA2000 and WLAN. In this method, illustrated in Fig.1, the baseband transmit signals generated by DSP using look-up tables (LUTs) based on the inverse of the nonlinearity characteristics of the power amplifier. The distorted signals are converted to analog signals by D/A converters and further converted to IF or RF by a quadrature modulator. To achieve perfect distortion cancellation, the reconstruction filters and modulator should be ideal.

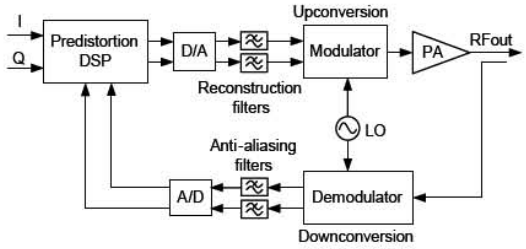

Fig.1. Block diagram of memoryless digital predistortion

However, analog implementations of the filters usually have non-zero passband ripple and non-constant phase delay [2]. Analog quadrature modulators suffer from gain and phase imbalance [3]. These nonideal factors can affect the predistortion cancellation results [4]. This paper gives an intuitive and quantitative analysis of the effects of the transmitter chain impairments on distortion cancellation results, and provides simulation to verify the analysis.

II. Filter Effects in Digital Predistortion Transmitters

A. Filter effects in transmitter chain

The filter effects in a digital predistortion transmitter are discussed in this section from a frequency domain point of view. In Fig.2 (a), the transmitter chain is ideal and all the nonlinearity (represented by the third order inter-modulation, IMD3, assuming a two tone input for simplicity) is generated by the PA only. The function of predistortion (PD) is to intentionally introduce some nonlinear predistorted sideband frequency components, which are intended to cancel the PA's nonlinear products. As shown in Fig.2 (b), at the output of the PA, if the sideband signals at the IMD3 frequencies generated by PD ("anti-IMD3") have equal amplitude but opposite phase with respect to the PA's initial IMD3, perfect cancellation can be achieved. However, in practical implementations, only finite cancellation can be accomplished.

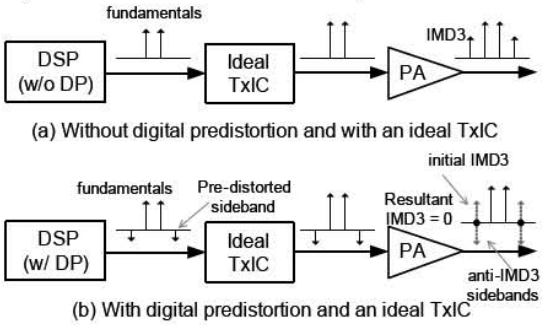

Fig.2. Schematic predistortion in a transmitter for two-tone inputs

Typically the analog implementation of the baseband reconstruction filter is of relative low order and finite bandwidth due to its complexity and cost in a transmitter

IC design, therefore it has some passband ripple and phase delay as illustrated in Fig.3.

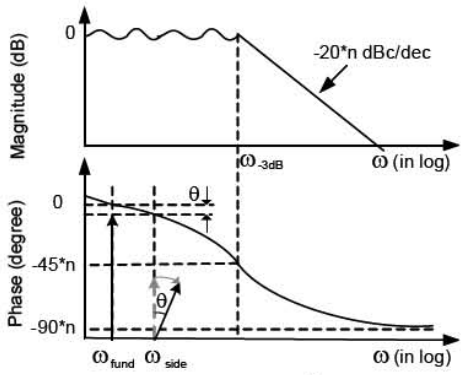

Fig.3. Magnitude and phase responses of n^{th}-order analog filter

When the filter is introduced in the transmitter chain (Fig.4), the fundamental and predistorted sideband components experience different amplitude and phase variations due to their frequency difference. Consequently, the IMD3 cancellation results are degraded.

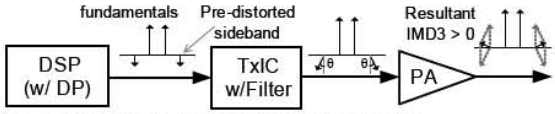

Fig.4. Filter effects in predistortion degradation

Vector analysis can be used to illustrate this cancellation degradation problem. In Fig.5, vectors A_1 and A_2 denote the amplitude and phase of the IMD3 and anti-IMD3 generated by the PA and the PD sidebands respectively for the case without a filter. The initial phase of A_1 is α and the phase difference of A_1 and A_2 is φ. The amplitude of the IMD3 after cancellation is A_3:

$$A_3 = \sqrt{A_1^2 + A_2^2 + 2A_1A_2\cos\varphi} \quad (1)$$

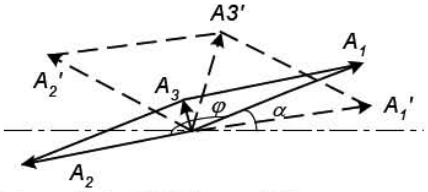

Fig.5. Vector analysis of IMD3 cancellation

The filter can change both the amplitude and phase of the fundamental and predistorted sideband components. For simplicity, we make several assumptions here. First, the baseband amplitude variation is ignored, which is reasonable since most designed filters have very small passband ripple usually less than 0.5dB. Second, there are no PM to AM and PM to PM distortions in the PA, which is also reasonable, if the PA is represented by a quasi-memoryless model. With these assumptions, the newly generated IMD3 and anti-IMD3 vectors A_1' and A_1' have the same amplitude as A_1 and A_2, but the phase difference between them is changed to $(\varphi - \theta)$ instead of φ due to the different phase shift θ within the passband of the filter shown in Fig.3. The amplitude of the new IMD3 after cancellation is A_3':

$$A'_3 = \sqrt{A'^2_1 + A'^2_2 + 2A'_1A'_2\cos(\varphi - \theta)} \quad (2)$$

Using (1) and (2), the cancellation degeneration results can be quantified.

B. Simulation of filter phase delay effects

The ADS harmonic balance (HB) simulation setup is shown in Fig.6. The input signals are two fundamental tones and two predistorted sideband tones. The PA is represented by a complex polynomial model created from an ADS PA design example [5]. The AM-AM and AM-PM curves are shown in Fig.7, where the matching between simulated data and 11^{th} order polynomial fitting is very good.

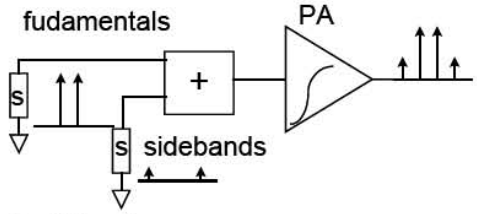

Fig.6. Simulation setup

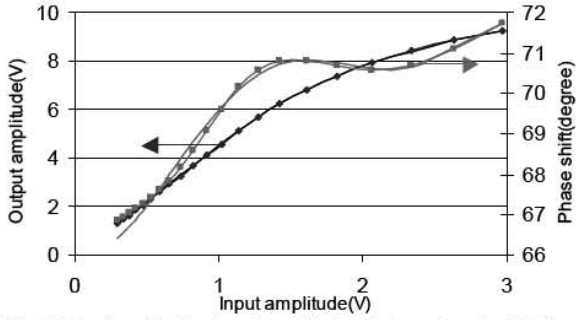

Fig.7. Simulated (w/markers) and fitting (w/o markers) of PA's AM-AM and AM-PM curves

The PA's initial IMD3 can be calculated by the two fundamental signals only. To achieve best cancellation results, the predistorted sideband tones are added with amplitude and phase of the optimal values determined from vector analysis. If the phase deviation of the input sideband tones occurs with respect to the optimal phase, the degradation of the cancellation can be seen. In Fig.8, the blue and red curves show the output IMD3 without PD and with optimal PD (ideal filter). The magenta and black

curves show the IMD3 with phase deviations of 15 and 30 degrees with respect to the optimal phase. The phase deviation values can be chosen corresponding to different filter characteristics, which is discussed in next sub-section. It can be seen that the cancellation degrades increasingly when the phase is further removed from the optimal phase.

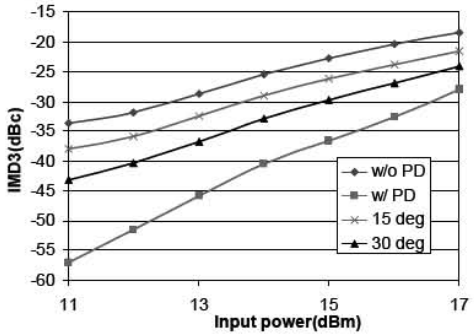

Fig.8. IMD3 cancellation of different phases vs Pin

C. Effects of filter types and parameters

The commonly used analog filters are Butterworth, Chebyshev and Elliptic types. Different filters have different passband and stopband properties. Even for a given filter type, parameters such as order and bandwidth can affect the amplitude and phase responses [2]. The bandwidth choice of the baseband reconstruction filter is a rather complex issue [6]. The principle is illustrated in Fig.9.

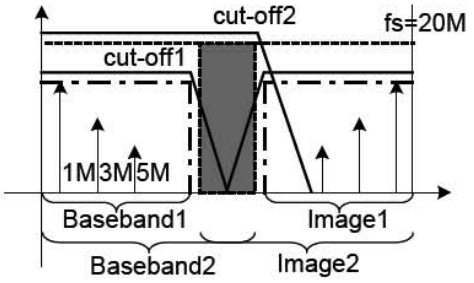

Fig.9. Filter cut-off frequency selection; Fundamental signal and its harmonics and sampling images are shown.

The filter should have a cut-off frequency f_c higher than the bandwidth of the input signal, which is 2MHz in our simulations denoted by f_b. But for predistortion applications, the cut-off frequency should be higher yet, due to the bandwidth expansion of the predistorted signal. In our simulations, we selected f_c high enough to pass at least the fifth order harmonic frequency components. However, the achievable cut-off frequency has an upper limit for a given D/A sampling rate (f_s) or over sampling ratio (OSR). For example, in Fig.9, the OSR is 10 (f_s =20MHz / f_b=2MHz). In the first case, the cut-off frequency is 8MHz and the passband to stopband transition region is 2MHz wide, thus the sampling image is within the stopband, and adequately attenuated. In the second case, the f_c is increased to 12MHz, and there is a significant interfering signal aliased into the baseband. Thus the rules of our filter cut-off frequency selection are: to pass the fifth order but to stop the sampling aliases.

First we study the IMD3 degradation for different cut-off frequencies with a fixed OSR of 12. According to our filter selection rules, the cut-off frequencies are 6MHz, 8MHz and 10MHz. The phase deviation (tabulated in Table1) and amplitude variation for different types of seventh order filters are calculated and by inserting these values into the simulation setup of Fig.6, we obtained the degraded IMD3 values shown in Fig.10.

	Butter-worth	Cheby (0.5dB)	Cheby (0.5dB)	Elliptic (0.5dB)
6MHz	75°	96.3°	89.9°	71°
8MHz	42.4°	53.8°	50.8°	40.7°
10MHz	19.4°	26.4°	23.6°	19.6°

Table1. Phase deviation of different filters vs cut-off frequency (OSR=12)

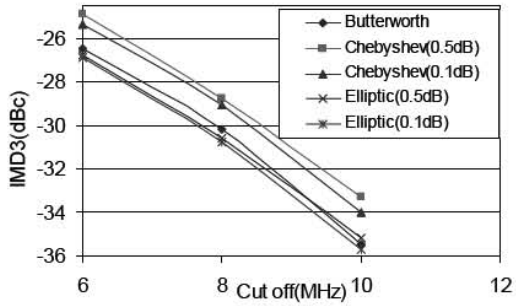

Fig.10. IMD3 degradation of different filters vs. cut-off frequency at Pin=13dBm (OSR=12)

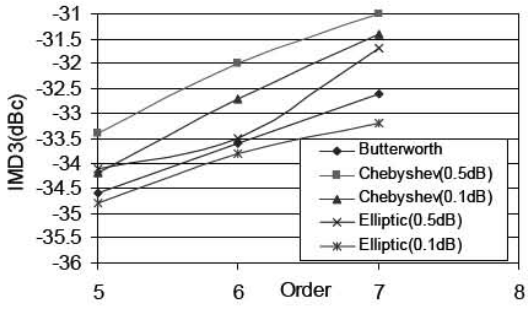

Fig.11. IMD3 degradation of different filters vs. filter order at Pin=13dBm (f_c=8MHz, OSR=10)

The conclusion drawn from Fig.10 is that if possible, a higher cut-off frequency filter should be used. However, to avoid sampling alias problems, higher OSR is then required, which may entail power consumption and complexity issues. Similarly, we studied the IMD3 degradation for different filter orders with a fixed cut-off of 8MHz and OSR of 10, as shown in Fig.11. It can be seen that lower order has a little better IMD3 cancellation, but the fact must be remembered that the stopband attenuation of lower order filters is poorer than that of higher order filters. From Fig.10 and Fig.11, we can see that the Elliptic filter with 0.1dB ripple and Butterworth filter are the best two filter candidates.

Compensation of the filter non-idealities cannot be accomplished with quasi-memoryless predistortion. However, predistortion that incorporates appropriates memory effect features (such as equalization filters as frequency domain compensator) could in principle be used to overcome these problems.

III. IQ IMBALANCE EFECTS IN DIGITAL PREDISTORTION TRANSMITTERS

It is important to maintain equal gains and 90-degree phase difference between the in-phase (I) and quadrature (Q) paths of the upconversion chain. Any disparity in gain and phase will yield amplitude and phase deviation from ideal values. I/Q imbalance can be quantified by transmitting a sine wave ($\sin \omega_{fk} t$) on the I path and a cosine wave ($\cos \omega_{fk} t$) on the Q path as shown in Fig.12,

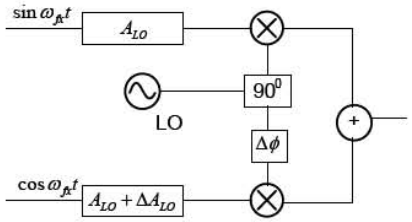

Fig.12. I/Q imbalance modulator

where the I path is assumed to be perfect for simplicity, and the Q path has amplitude and phase errors of ΔA_{LO} and $\Delta\phi$. At the output the upconverter, the amplitude A_{LO-fk} at the desired single side band frequency $\omega_{LO} - \omega_{fk}$ is found to be

$$\left|A_{LO-fk}\right|^2 = A_{LO}^2\left(1 + \Delta A_{LO-fk}\right) \quad (3)$$

where the output amplitude error ΔA_{LO-fk} is obtained as

$$\Delta A_{LO-fk} = \frac{\cos\Delta\phi - 1}{2} + \frac{\Delta A_{LO}}{2A_{LO}}\left(1 + \cos\Delta\phi\right) \quad (4)$$

In Fig.13, due to the I/Q imbalance, the fundamental ω_{f1} and predistorted sidebands ω_{f3} experience same percent amplitude variation after the modulator. At the output of the PA, the amplitude variation of the "anti-IMD3" generated by PD is proportional to the variation of sidebands at the input of PA, because the predistorted sidebands are very small and not distorted by the PA. However, the amplitude variation of the fundamental tones generates a cubic amplitude variation and phase deviation of IMD3 at the output of PA. As a result, the IMD3 cancellation is degraded due to the different amplitude and changing phase of the PA's IMD3 and PD's "anti-IMD3" components.

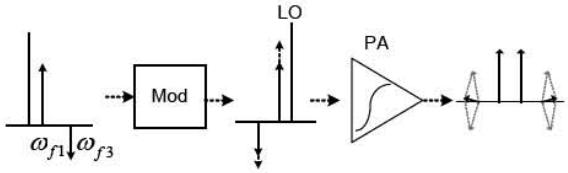

Fig.13. IMD3 degradation due to I/Q imbalance modulator

In general, I/Q imbalance can compensated digitally [3] with low expense and high precision.

IV. SUMMARY

Nonideal reconstruction filter and I/Q imbalance effects on digital predistortion have been studied. Mathematical analysis and simulation have been carried out to identify proper predistortion compensation methods.

REFERENCES

[1] J. Muhonen, M. Kavehrad and R. Krishnamoorthy, "Look-Up Table Techniques for Adaptive Digital Predistortion: A Development and Comparison," IEEE *Trans. MTT.*, Vol 49, no. 5, pp. 1995-2002, Sep. 2000.

[2] R. Scchaumann and M. E. Van Valkenburg, Design of Analog Filters. New York: Oxford, 2000.

[3] J. K. Cavers and M. W. Liao, "Adaptive compensation for Imbalance and Offset Losses in Direct Conversion Transceivers," IEEE *Trans. Vehicular Technology,* Vol 42, no. 4, pp. 581-588, Nov. 1993.

[4] L. Sundstrom, M. Faulkner and M. Johansson, "Effects of Reconstruction Filters in Digital Predistortion Linearizers for RF Power Amplifiers," IEEE Trans. Vehicular Technology, Vol 44, no. 1, pp. 131-139, Feb. 1995.

[5] Agilent ADS 2004A, "Examples\BehavioralModels\ AmpP2D_prj\Motorola_PA"

[6] V. W. Leung, L. E. Larson and P. S. Gudem, "Improved Digital-IF Transmitter Architecture for Highly Integrated W-CDMA Mobile Terminals," IEEE *Trans. Vehicular Technology,* Vol 54, no. 1, pp. 20-32, Jan. 2005.